Clay Minerals (2019), **54**, 369–377
doi:10.1180/clm.2019.49

CAMBRIDGE UNIVERSITY PRESS

Article

Mineralogical study of clays from Dobrodo, Serbia, for use in ceramics

Maja Milošević[1]*, Predrag Dabić[1], Sabina Kovač[1], Lazar Kaluđerović[2] and Mihovil Logar[1]

[1]University of Belgrade, Faculty of Mining and Geology, Belgrade, Serbia and [2]University of Belgrade, Faculty of Agriculture, Belgrade, Serbia

Abstract

This study focuses on the mineralogical characterization of four raw clay samples from Dobrodo deposit, Serbia. Several analytical methods were applied to determine the chemical and mineralogical composition, morphology and physical properties (colour, plasticity, specific surface area, particle size and cation-exchange capacity) of the clay samples. Kaolinite, smectite and illite are the predominant phases in all of the samples studied that contain between 60.2 and 87.1 wt.% of clay. Quartz, feldspars, paragonite and Ti- and Fe-bearing phases were also identified. The relatively high SiO_2/Al_2O_3 mass ratio indicates abundant quartz. The cation-exchange capacity of the samples varied between low and moderately charged clay minerals (12–52 mmol 100 g^{-1}) with specific surface area values ranging from 94 to 410 m^2 g^{-1}. The plasticity index values (11–23%) suggest low to moderate plasticity. Preliminary results show that most of the raw clay from Dobrodo deposit might be suitable for use in ceramic applications.

Keywords: ceramics, clay, Dobrodo, mineralogy, raw material, Serbia

(Received 14 May 2019; revised 23 September 2019; Accepted Manuscript online: 11 October 2019; Associate Editor: Joao Labrincha)

Clays are commonly used materials in ceramics (Norton, 1970; Reeves *et al.*, 2006; Murray, 2007) as well as in cosmetic, medical and environmental applications (Bundy & Ishley, 1991; Murray, 1991; Minato & Shibue, 1999; Murray & Kogel, 2005; Viseras *et al.*, 2007). Raw clays have complex chemical, mineralogical and physical properties that may be useful in manufacturing processes (*e.g.* Felhi *et al.*, 2008; Mitrović *et al.*, 2009; Hammami-Ben Zaied *et al.*, 2015; Boussen *et al.*, 2016; Milošević & Logar, 2017; Milošević *et al.*, 2017; Tsozué *et al.*, 2017, *etc.*). Clays often contain impurities, most commonly calcite, quartz, feldspars and iron oxides. Clay materials have been used worldwide in traditional handcrafting without chemical pretreatments. Clays that are used in the manufacture of structural bricks and tiles are often processed directly as they are dug out from the ground. In their untreated form, these raw clays are easily workable because they already contain fillers and fluxes in association with the clay minerals. In the case of ceramics and whitewares, for which the clay material should be relatively pure, the clays need to be treated to remove most impurities.

The clay deposit in the village of Dobrodo, Serbia, has traditionally been exploited by small manufacturers of ceramics for >400 years and is used in the production of the renowned Zlakusa pottery. The location of this deposit in relation to the pottery makers in the village of Zlakusa is of great importance to ethnological and archaeological research (Djordjević, 2013). Nevertheless, its mineralogy, locality and application potential remain little known worldwide, especially within the scientific community. The main aim of the present study was to characterize mineralogically and determine the impurities contained within the Dobrodo raw clay deposit.

*Email: maja.milosevic@rgf.bg.ac.rs

Cite this article: Milošević M, Dabić P, Kovač S, Kaluđerović L, Logar M (2019). Mineralogical study of clays from Dobrodo, Serbia, for use in ceramics. *Clay Minerals* **54**, 369–377. https://doi.org/10.1180/clm.2019.49

Geological and geographical setting

The Dobrodo clay deposit is located in the village of Vranjani, ~185 km from Belgrade, Serbia's capital city. It is operated by a private contractor and the clay mixture has only been used for traditional pottery-making. The clay is mined from pits that are opened afresh each year. To reach layers of high-quality clay, an overburden layer ~3 m thick must be removed because the surface water drains in the clay pit, rendering it useless until the dry summer period of the year. The deposit is mostly of Miocene age, consisting mainly of sand, clay, marl and dolomite (Fig. 1). The Miocene formations begin with sandstone or sand and conglomerate and were deposited in freshwater basins. The sediments have a thin-layered, fine, pelite structure, often with fine lamination and occasional lenses and concretions (Mojsilović *et al.*, 1971).

Experimental

Materials

The clay was collected from exposed faces of the Dobrodo deposit, which consists of several discrete layers (Fig. 2). The thin layer of clay at the top of the deposit has a brown colour (sample 6) and contains lens-like inclusions of light beige-coloured material (sample 5). Between the upper part and the thickest light-grey layer at the bottom (sample 3) lies a thin stratum of dark-grey clay with a distinct coal-like odour (sample 4). Representative samples were collected according to their colour and depth. Approximately 1 kg of each sample (four samples in total) was dried at room temperature, crushed and homogenized without further separation or purification.

Analytical methods

Grain-size distribution was determined by the pipette method on raw samples according to the DIN ISO 11277 (2002). The X-ray

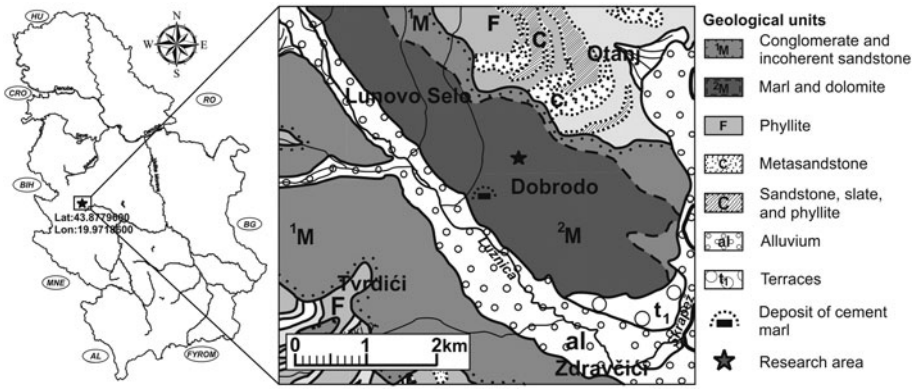

Fig. 1. Location (left, black star) and geological setting of the Zlakusa clay deposit (right, black star) (Basic Geological Map of Serbia 1:100,000, Titovo Užice sheet).

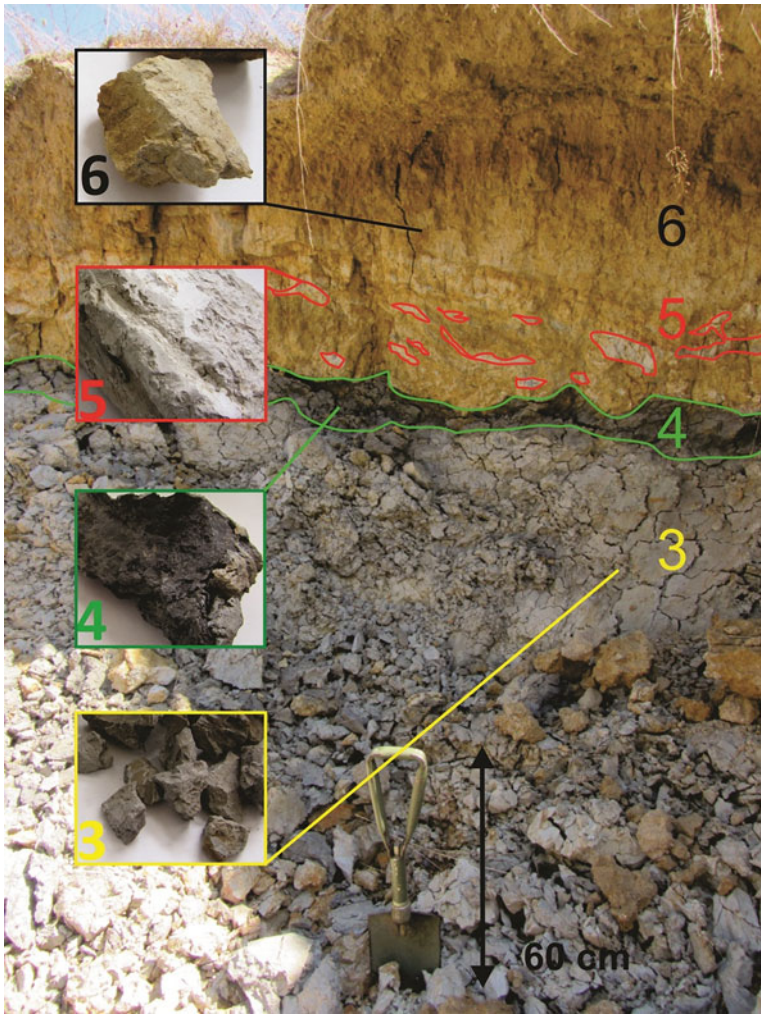

Fig. 2. Layers of the Dobrodo deposit with investigated samples and their corresponding labels.

powder diffraction (XRPD) data were collected on a Rigaku SmartLab X-ray powder diffractometer at room temperature using Bragg–Brentano geometry and Cu-$K\alpha$ radiation. The diffractometer was operated at 40 kV and 30 mA in the scan range of 3–70°2θ with a step size of 0.01°2θ and scanning speed of 2°2θ min^{-1}. The XRPD experiments were carried out on powdered bulk samples and on oriented preparations that were air dried (N), solvated with ethylene glycol (EG) and heated to 550°C for 1 h (H). The mineral phases were identified using Rigaku *PDXL 2* software and the PDF-2 database (International Centre for Diffraction Data). The mass ratios of the clay mineral phases present were determined with the whole-powder pattern fitting method (WPPF) using the same software.

The chemical compositions of the samples were determined by energy-dispersive X-ray fluorescence (ED-XRF) using an Oxford 2000 ED-XRF spectrometer equipped with *XpertEase* software.

https://doi.org/10.1180/clm.2019.49 Published online by Cambridge University Press

Table 1. Chemical analysis of the samples (wt.%).

Sample	SiO_2	Al_2O_3	Na_2O	K_2O	CaO	MgO	Fe_2O_3[a]	TiO_2	MnO	LOI	Total
6	64.80	18.07	1.13	0.91	0.42	0.03	4.42	0.90	0.02	9.19	99.89
5	69.90	19.07	0.05	0.98	0.45	0.04	2.68	0.50	0.02	6.17	99.86
4	61.57	16.71	0.05	0.35	0.52	0.32	2.53	0.22	0.03	17.49	99.79
3	66.53	14.80	0.08	0.05	0.32	0.05	2.14	0.18	0.03	15.60	99.78

[a] Total Fe as Fe_2O_3.
LOI = loss on ignition (950°C).

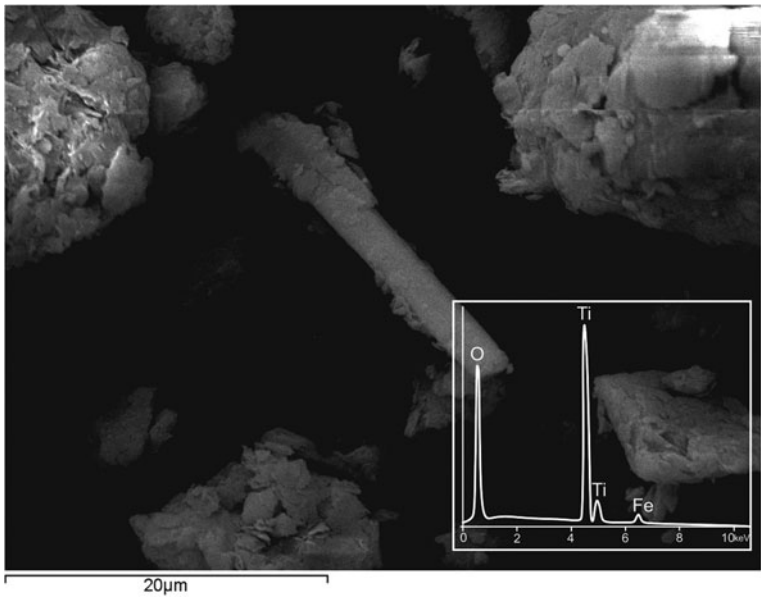

Fig. 3. SEM images of rutile minerals, with insert showing corresponding energy-dispersive X-ray spectra.

The samples (10 g) were ground in a HERZOG HSM 100H vibrational mill for 30 s to pass through a 160 µm sieve. Metal sample holders were filled with boric acid powder over which the samples were evenly distributed and then pressed (10 s) in a T-40 SPECAC press to form 40 mm pellets. The cation-exchange capacity (CEC) of the samples was determined after saturation with methylene blue solution according to ASTM C 387-99 (1984), using a uniSPEC2 spectrophotometer. Visual inspection of the sample colour was conducted using the geological rock colour chart with genuine Munsell colour chips (Geological Society of America, 2009). The dominant wavenumbers of the dry, pressed, raw powder samples before and after firing at 1100°C were measured with diffuse reflectance apparatus (400–700 nm) using a CCS200 spectrometer (Thorlabs) according to the Commission Internationale de l'Eclairage (1932).

Differential thermal analysis (DTA) was performed on a modernized ADAMEL furnace equipped with a Pt–PtRh thermocouple and BK PRECISION XLN15010 DC power supply as the heating rate controller in an air atmosphere. The heating rate was 10°C min^{-1} over a temperature range of 20–1100°C. Measured data were plotted relative to a baseline obtained using Al_2O_3 as a reference material. Particle morphology and grain-size distribution were determined by scanning electron microscopy (SEM) with a JEOL JSM-6610LV scanning electron microscope coupled with an Oxford X-Max 20 mm^2 energy-dispersive X-ray spectrometer. The Atterberg limits (Atterberg, 1911) were determined according to the Casagrande method (Laboratoire Central des Ponts et Chaussées, 1987).

Results and discussion

Chemical composition

Chemical analysis of the samples (Table 1) shows a relatively large abundance of SiO_2 (>61 wt.%) and Al_2O_3 (16–19 wt.%), a total Fe_2O_3 content of 2–4% and a small K_2O content (0.05–1.00%). The mass ratio of SiO_2/Al_2O_3 ranges from 3.58 to 4.49, which is significantly greater than the values generally found in pure kaolinite (1.18) and pure montmorillonite (2.36) (Boussen *et al.*, 2016). The high values of the SiO_2/Al_2O_3 mass ratios are attributed to the excess of quartz and the presence of illite. The ideal composition of kaolinite is SiO_2 46.5 wt.%, Al_2O_3 39.5 wt.% and H_2O 13.96 wt.% (Newman, 1987), which confirms that the studied samples have greater SiO_2 contents. The loss on ignition of the samples is associated with the presence of hydroxides, organic matter and clay minerals (Baccour *et al.*, 2009), which is confirmed by DTA. The small amounts of Ca and Mg oxides indicate the lack of carbonate minerals. Hence, the samples may be regarded as carbonate-free and SiO_2-rich, which makes them suitable for ceramic products. The low abundance of K_2O and Na_2O might indicate further the presence of kaolinite minerals in the samples that naturally contain a small amount of flux materials (Monterio & Vieira, 2004; Celik, 2010). Samples 3 and 4 contain the smallest amounts of $K_2O + Na_2O$ (0.13 and 0.40 wt.%, respectively), indicating a greater degree of kaolinization (Sikalidis *et al.*, 1989; Kamseu *et al.*, 2007). Fe_2O_3, TiO_2 and Na_2O are more abundant in the uppermost sample (#6) than in the lowermost sample (#3; Table 1).

https://doi.org/10.1180/clm.2019.49 Published online by Cambridge University Press

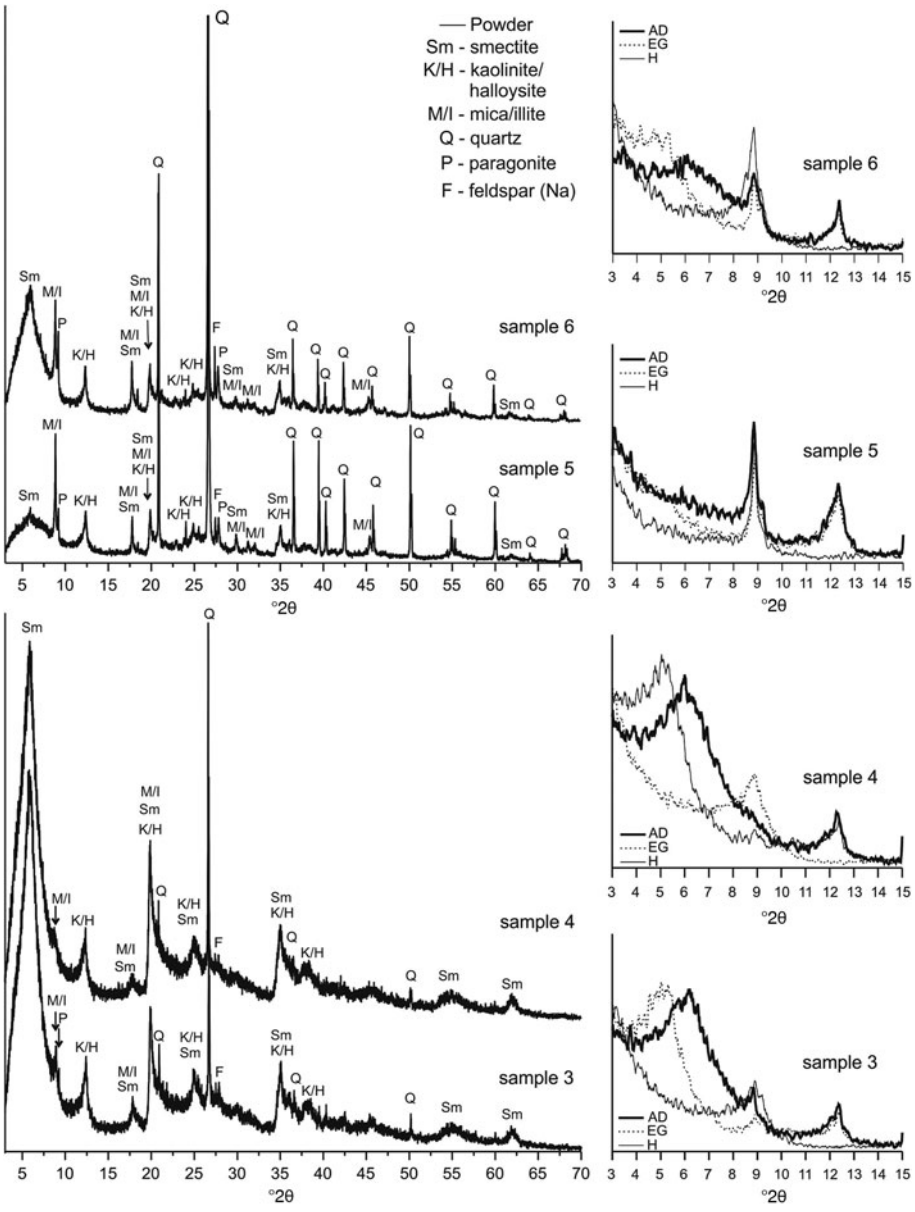

Fig. 4. XRPD traces of the raw samples (left) and oriented clay fractions of the samples (right).

Table 2. Relative contributions of phases obtained by the WPPF method.

	Sample			
	6	5	4	3
Quartz	+++	+++	+	+
Smectite	+	*	+++	+++
Kaolinite/halloysite	+++	+	+++	+++
Mica/illite	++	++	+	+
Na-feldspar	+	+	+	+
Paragonite	+	+	*	*

+++ = dominant; ++ = moderate; + = small amount; * = accessory.

Table 3. Mass ratios of the clay mineral phases obtained by the WPPF method.

	Sample			
	6	5	4	3
Kaolinite/halloysite	71	71	34	31
Smectite	18	2	51	51
Mica/illite	11	27	15	18

Iron-bearing phases were not detected unambiguously by XRPD analysis in most samples, indicating that Fe may be present in an amorphous form. Titanium precipitates quickly *in situ* (Bain, 1976). The TiO_2 content does not exceed 0.90% in any of the samples, and the corresponding minerals detected by SEM were needle-like crystals of rutile (Fig. 3), indicating slight weathering of the soil (Sherman, 1952).

Mineralogy

The mineral phases identified in the XRPD traces are smectite (International Centre for Diffraction Data #01-073-6746), kaolinite/halloysite (01-078-2110), mica/illite (01-078-5138), quartz (01-085-0930), paragonite (01-075-1202) and Na-feldspar (albite)

https://doi.org/10.1180/clm.2019.49 Published online by Cambridge University Press

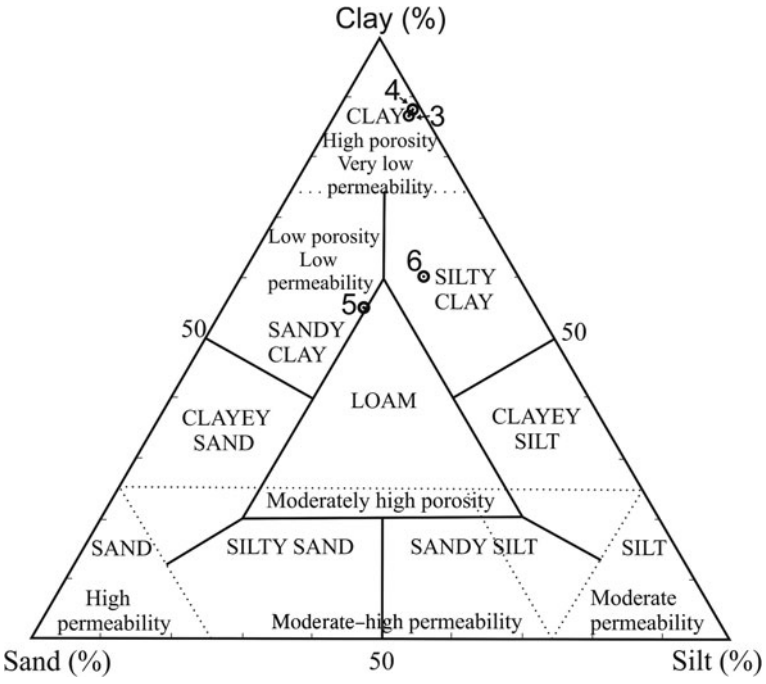

Fig. 5. Ternary diagram of the samples showing the relationship between clay, silt and sand (after McManus, 1988; Strazzera *et al.*, 1997).

(01-076-0803). Kaolinite/halloysite and mica/illite minerals were identified by the reflections at 7.2 and 10 Å, respectively, in the bulk XRPD traces (Fig. 4) and are not affected by EG solvation (Fig. 4). The intensity of the kaolinite 001 reflections decreased after heating (Fig. 4). Swelling minerals, such as smectite, exhibit their 001 reflection in the <7 Å region, which shifts to lower angles after EG solvation (Fig. 4).

Semi-quantitative estimates of the mineral phases present are shown in Table 2. The dominant mineral phases in samples 3 and 4 are smectite and kaolinite (Fig. 4, Table 2). Illite is present in small amounts when compared to smectite and kaolinite (Table 3). Minor phases are quartz, Na-feldspar and accessory paragonite. In samples 5 and 6 the dominant phase is quartz (Fig. 4, Table 2). Other phases are clay minerals, Na-feldspar and paragonite. Among the clay minerals, kaolinite is the most dominant phase (~70 wt.%). Sample 5 has the smallest amount of smectite compared to the remaining samples. The illite content is virtually constant among the clay minerals (11–18 wt.%), being greatest in sample 5. The abundance of Na-feldspars decreases slightly with depth, being greatest in sample 6 and smallest in sample 3 (Fig. 4).

The mass ratios of the present clay mineral phases normalized to 100 wt.%, as obtained by the WPPF method, are shown in Table 3. These results separate samples 6 and 5 with a greater kaolinite content from samples 3 and 4, which are dominated by smectite.

Particle-size distributions

The particle-size distribution of clay plays an essential role in defining the properties of suspensions (plasticity, viscosity) and green pastes during drying and firing (Rivi & Ries, 1997), with particular attention given to the finer fraction (<2 μm) for ceramic products (Mahmoudi *et al.*, 2008). The tested samples contained 60.2–87.1 wt.% clay, 10.9–26.1 wt.% silt and 1.2–25.6 wt.% sand fractions. Samples 3 and 4 are rich in fine particles (87.0 and 87.1 wt.%, respectively), while sample 5 contains more coarse particles (25.6 wt.% between 2.00 and 0.06 mm). The proportions of clay, silt and sand fractions were plotted on a ternary diagram (McManus, 1988; Strazzera *et al.*, 1997) to evaluate sample permeability (Fig. 5). Samples 3 and 4, which have the highest percentages of clay fractions, have high porosity and very low permeability. In addition, samples 5 and 6, which are classified as sandy clay and silty clay, respectively, have low porosity and low permeability. High permeability leads to low cohesion and implies difficulties in the extrusion processes (El Ouahabi *et al.*, 2014).

Scanning electron microscopy

The SEM images of the samples show that kaolinite occurs as lamellar hexagonal flakes of 2–10 μm in diameter with broken edges (Fig. 6), occasionally forming booklets. Tubular crystals 2–7 μm long are common, confirming the presence of halloysite (Fig. 6). The morphology of a tubular halloysite may result from alteration of platy kaolinite particles or be derived from feldspars and micas (Singh & Gilkes, 1992; Joussein *et al.*, 2005). Tubular particles are relatively Fe- and Ti-poor, while larger amounts of Fe form a platy halloysite morphology (Joussein *et al.*, 2005). The morphology of the samples studied suggests that the second major clay mineral is montmorillonite. Montmorillonite consists of thin, crumbled plates 2–20 μm in size with undefined outlines and large aggregates with a significant surface area. A small quantity of illite appears in the form of fibres and laths, suggesting precipitation from formation waters in sandstones (Güven, 2001).

The Ti-bearing phase in the studied samples is rutile, consisting of elongate and needle-like crystals 2–20 μm long. The rutile has a small Fe content (Fig. 3). The abundance of rutile is greatest in sample 6 and only a couple of grains were observed in sample 3, which is in accord with the TiO_2 contents obtained by XRF analysis. A few irregular Fe oxide grains of rounded shape have also been observed in sample 4.

https://doi.org/10.1180/clm.2019.49 Published online by Cambridge University Press

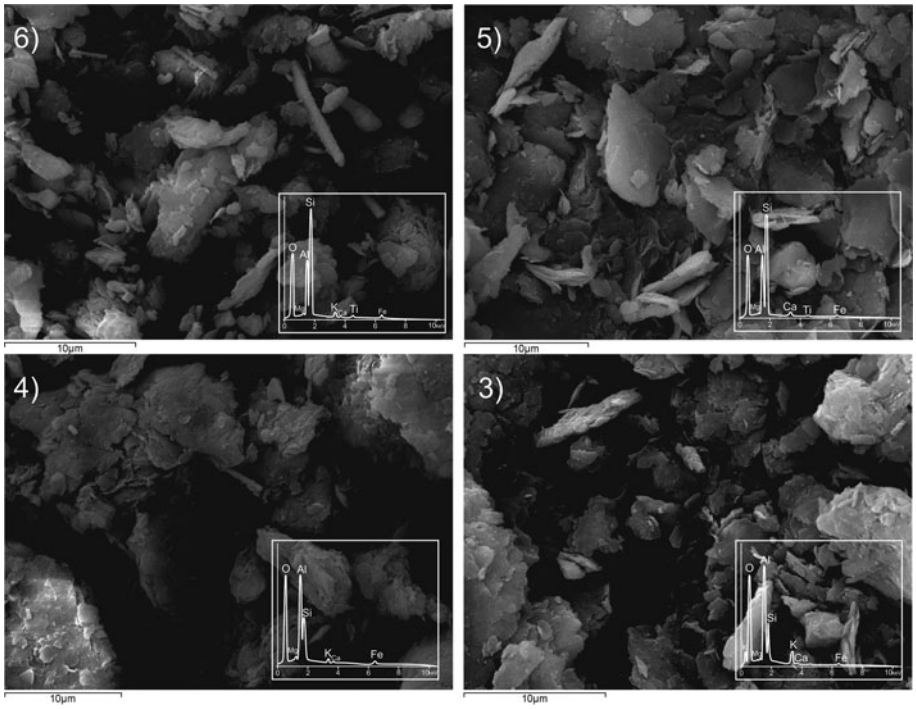

Fig. 6. SEM images of the investigated samples, with inserts of energy-dispersive X-ray spectra.

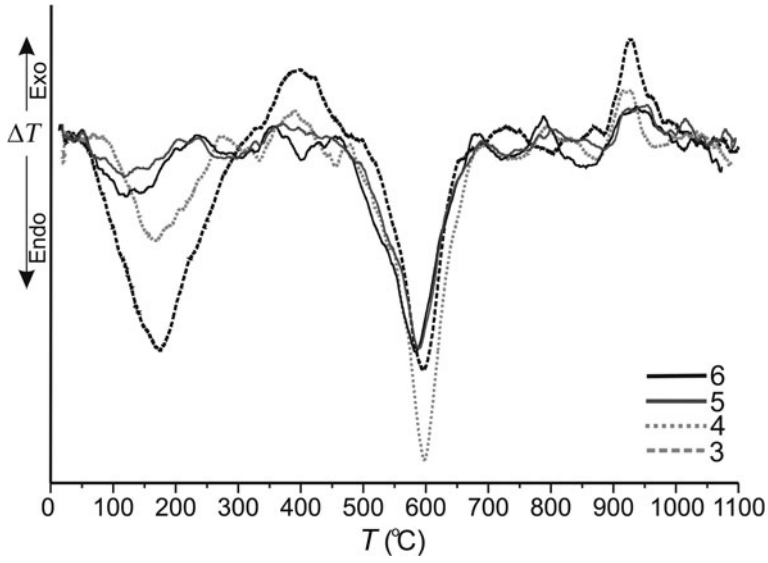

Fig. 7. DTA curves of the investigated samples.

Thermal analysis

The DTA curves of all of the clay samples show distinct endothermic peaks (Fig. 7). The first endothermic event between 100 and 200°C corresponds to the loss of adsorbed and interlayer water (Greene-Kelly, 1957; Földvári, 2011). In samples 3 and 4, this band is broad and covers a region between 50 and 300°C, indicating the presence of several layer silicates – illite, kaolinite, halloysite and montmorillonite (Földvári, 2011). The endothermic peaks at ~350 and 450°C correspond to the dehydration of goethite (Grim & Rowland, 1944) and probably of halloysite (Norton, 1939; Grim & Rowland, 1944). The exothermic peak at ~400°C corresponds to the development of α-Fe_2O_3 from 'protohematite' (Földvári, 2011) and/or the presence of organic matter (Yariv, 2003). Kaolinite dehydroxylates to metakaolinite at 500–600°C.

Table 4. CEC and SSA values of the studied samples compared to mixtures of clay minerals according to Arab *et al.* (2015).

Sample	CEC (mmol 100 g^{-1})	SSA (m^2 g^{-1})	Sample[a] (%)		CEC[a] (mmol 100 g^{-1})	SSA[a] (m^2 g^{-1})
			Kaolinite	Bentonite		
6	22.4	175.8	80	20	27.7	216.5
5	12.0	93.8	90	10	16.4	128.4
4	52.4	410.4	50	50	60.0	469.8
3	45.2	353.6	60	40	49.9	390.9

[a] Values obtained from Arab *et al.* (2015).

Halloysite also has a characteristic endothermal reaction due to dehydroxylation to metahaloysite (530–590°C) and illite dehydroxylates at 550°C (Norton, 1939; Speil *et al*, 1945; Földvári,

https://doi.org/10.1180/clm.2019.49 Published online by Cambridge University Press

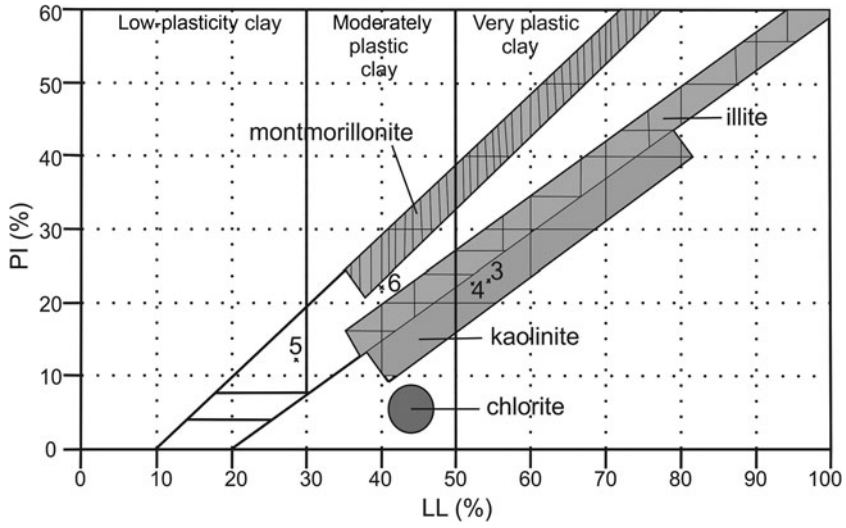

Fig. 8. Holtz & Kovacs (1981) diagram of the studied samples. LL = liquid limit; PI = plasticity index.

2011). The endothermic peaks at 650–700°C correspond to Ca-montmorillonite, hydromuscovite/illite and pyrophyllite. The broad endothermic peak at ~820°C indicates deconstruction of the silicate lattice and suggests the presence of a mixed-layer component in the clay sample, such as illite-smectite (Earnest, 1991). Structural decomposition of Ca-montmorillonite and crystallization of mullite, Mg-spinel and cristobalite occur at >850°C (Földvári, 2011) in the form of a doublet of endo-exothermic reactions. The new crystalline phase in the samples at ~950°C is primary mullite or pseudomullite with a Si-Al spinel structure and amorphous $SiO_2 + \gamma\text{-}Al_2O_3$ (Speil *et al.*, 1945; Földvári, 2011). The presence of ferric oxides on the surfaces of the particles reduces the size and intensity of this band.

Specific surface area and CEC

The CEC is defined as the amount of exchangeable cations, and it represents important information in evaluating the quality of clays (Burrafato & Miano, 1993). The CEC of the samples varied between 12 and 52 mmol 100 g^{-1}, while specific surface area (SSA) ranges from 94 to 410 m^2 g^{-1} (Table 4). Greater CEC values (80–150 mmol 100 g^{-1}; Grim, 1953) indicate greater swelling capacity, which is typical of the smectite group of minerals. The kaolin minerals have CEC values in the range of 3–15 mmol 100 g^{-1}; hence, sample 5 might be described as a predominantly kaolinite clay (Grim, 1953). Samples 3, 4 and 6 do not follow the CEC limits set by Grim (1953). When compared to mixtures of clay minerals in previous studies (Arab *et al.*, 2015), an obvious pattern is observed (Table 4). Samples with smaller CEC values contain more kaolinite. Moderate amounts of kaolinite and smectite yield larger CEC values compared to pure kaolinite, but lower CEC values than bentonite clays (>70 mmol 100 g^{-1}).

Plasticity and toughness

The liquid limit (LL) of the samples varies from 32.4% to 53.6% and the plastic limit (PL) varies from 13.8% to 30.2%. Clays with a plasticity index (PI) <10% are not appropriate for building-related products and those with a plasticity index >34% would be difficult to extrude (Barnes, 2014). Projection of the samples onto the diagram of Holtz & Kovacs (1981) (Fig. 8) shows that the PI varies from 11.7% to 23.4%. Samples 3 and 4 are classified as very plastic clays, sample 6 as moderately plastic and sample 5 is a low-plasticity clay. The presence of smectite, even in small amounts, may significantly affect plasticity.

The PI/LL ratio is highly correlated with toughness (kJ m^{-3}), which represents the ability of clay to be deformed (Moreno-Maroto & Alonso-Azcárate, 2018). Toughness refers to the work per unit volume required to cause deformation on the sample when it is rolled (Barnes, 2009, 2013a, 2013b; Moreno-Maroto & Alonso-Azcárate, 2018). According to their maximum toughness (T_{max}) values, samples can be divided into two groups (Barnes, 2009, 2013a, 2013b). Samples 3, 4 and 5 have T_{max} values of 13, 11 and 9 kJ m^{-3}, respectively, and may be classified as moderately tough, and sample 6 may be considered as a highly tough and plastic clay with a T_{max} value of 25 kJ m^{-3}.

Colour properties

The colour properties include observed colour (Munsell colour chart), colour values (nm) and purity of the colour (%) for raw and fired samples (1100°C). The colour of the raw clay is determined by the mineralogical composition and its position in the stratigraphic sequence. The colour of sample 6 from the uppermost horizon is greyish–yellow (5Y8/4), sample 5 is moderately orange–yellow (7.5YR7/8), sample 4 is greyish–brown (5Y3/2) and sample 3 is moderately yellowish–brown (10YR5/4). The dominant wavelengths of the original samples and in the samples after firing at 1100°C are shown in Table 5. Colouration is not due solely to the Fe_2O_3 content, as other constituents such as MnO and TiO_2 may also modify the final colour of the product (Kreimeyer, 1987; Celik, 2010; Dondi *et al.*, 2014; Boussen *et al.*, 2016).

The purity of the colour is greater after firing of the samples (Table 5). In addition, samples have a significantly darker colour after firing compared with their raw counterparts. Samples containing 1–5% Fe_2O_3 would acquire a light-brown colour after firing (Murray, 2007). Colour changes to darker shades upon heating treatment due to the formation of hematite. The colour of the fired bodies depends on the Fe oxide content, and the limit of 3 wt.% of Fe_2O_3 has been found to be the value that separates light from dark firing bodies (Dondi *et al.*, 2014).

https://doi.org/10.1180/clm.2019.49 Published online by Cambridge University Press

Table 5. Dominant wavelength (nm) and purity of the colour (%) of raw samples and samples after firing.

	Sample			
Raw samples	6	5	4	3
Dominant wavelength	581.7	579.8	588.6	581.3
Purity of the colour	22.7	10.9	6.8	10.9
Fired samples				
Dominant wavelength	585.7	589.3	588.4	589.6
Purity of the colour	85.9	95.2	87.3	88.4

Summary and conclusions

The clay samples from the Dobrodo deposit consist mainly of smectite, kaolinite/halloysite and illite. Quartz, feldspars, minor goethite and acicular rutile are present as non-clay minerals. The tested samples contained between 60.2 and 87.1 wt.% clay, between 10.9 and 26.1 wt.% silt and between 1.2 and 25.6 wt.% sand fractions. The sample colour ranges from greyish-yellow to moderately yellowish-brown, although after firing the colours become considerably darker. The clays are relatively rich in SiO_2 and Al_2O_3, with SiO_2/Al_2O_3 mass ratios ranging from 3.58 to 4.49 wt.% due to the presence of excess quartz in the samples. The Fe_2O_3, TiO_2 and Na_2O contents are increased in the uppermost layers of the deposit (sample 6) compared to the lowermost layers. The samples consist mostly of kaolinite flakes, tubular halloysite, minor illite and smectite. The CEC values of the samples vary between 12 and 52 mmol 100 g^{-1}, while the SSA ranges from 94 to 410 m^2 g^{-1}. Regarding plasticity, samples 3 and 4 may be described as very plastic and moderately tough clays, sample 6 as a moderately plastic and highly tough clay and sample 5 as a moderately tough and low-plasticity clay.

The most suitable application of the clay from Dobrodo deposit is the manufacture of pottery. Further research and additional fieldwork should be extended to other areas of the Dobrodo deposit to explore clay-rich zones and to investigate the possibilities of the commercial applications of these raw clays.

Acknowledgements. The present study was supported by the Ministry of Education, Science and Technological Development of the Republic of Serbia, Project no. 176010. The authors acknowledge the SEM laboratory at the University of Belgrade, Faculty of Mining and Geology, Department of Mineralogy, Crystallography, Petrology, and Geochemistry.

References

Arab P.B., Araújo T.P. & Pejon O.J. (2015) Identification of clay minerals in mixtures subjected to differential thermal and thermogravimetry analyses and methylene blue adsorption tests. *Applied Clay Science*, **114**, 133–140.

ASTM C 837-99 (1984) *Standard Test Method for Methylene Blue Index of Clay (C 837-99). 1984 Annual Book of ASTM Standards, sect. 15, vol. 15.02*. Philadelphia, PA, USA, American Society for Testing and Materials (ASTM).

Atterberg A. (1911) Die Plastizität der Tone. *Internationale Mitteilungen der Bodenkunde*, **I**, 4–37.

Baccour H., Medhioub M., Jamoussi F. & Mhiri T. (2009) Influence of firing temperature on the ceramic properties of Triassic clays from Tunisia. *Journal of Materials Processing Technology*, **209**, 2812–2817.

Bain D.C. (1976) A titanium-rich soil. *Journal of Soil Science*, **27**, 68–70.

Barnes G.E. (2009) An apparatus for the plastic limit and workability of soils. *Proceedings Institution of Civil Engineers*, **162** (3), 175–185.

Barnes G.E. (2013a) An apparatus for the determination of the workability and plastic limit of clays. *Applied Clay Science*, **80–81**, 281–290.

Barnes G.E. (2013b) *The Plastic Limit and Workability of Soils*. PhD thesis, University of Manchester, 427 pp.

Barnes G. (2014) The workability of natural clays and clays in the ceramics industry. Pp. 183–202 in: *Clays and Clay Minerals: Geological Origin, Mechanical Properties and Industrial Applications* (L.R. Wesley, editor). Hauppauge, NY, USA, Nova Science Publishers.

Boussen S., Sghaier D., Chaabani F., Jamoussi B. & Bennour A. (2016) Characteristics and industrial application of the Lower Cretaceous clay deposits (Bouhedma Formation), Southeast Tunisia: potential use for the manufacturing of ceramic tiles and bricks. *Applied Clay Science*, **123**, 210–221.

Bundy W.M. & Ishley J.N. (1991) Kaolin in paper filling and coating. *Applied Clay Science*, **5**, 397–420.

Burrafato G. & Miano F. (1993) Determination of the cation exchange capacity of clays by surface tension measurements. *Clay Minerals*, **28**, 475–481.

Celik H. (2010) Technological characterization and industrial application of two Turkish clays for the ceramic industry. *Applied Clay Science*, **50**, 245–254.

Commission Internationale de l'Eclairage (1932) *1931 Commission Internationale de l'Eclairage Proceedings. Huitième session*. Pp. 19–29. Cambridge, UK, Cambridge University Press.

DIN ISO 11277 (2002) *Deutsches Institut für Normung. Bodenbeschaffenheit – Bestimmung der Partikelgr ßenverteilung in Mineralb den*. Berlin, Germany, Beuth.

Djordjević B. (2013) Pottery making in Zlakusa. First ethnoarchaeological research project in Serbia. P. 49 in: *Conference Proceedings, Rome, Italy, 13th–14th May 2010, BAR International Series 2472*. Oxford, UK, Archaeopress.

Dondi M., Raimondo M. & Zanelli C. (2014) Clays and bodies for ceramic tiles: reappraisal and technological classification. *Applied Clay Science*, **96**, 91–109.

Earnest C.M. (1991) Thermal analysis of selected illite and smectite clay minerals. Part I. Illite clay specimens. *Thermal Analysis in the Geosciences*, **38**, 270–286.

El Ouahabi M., Daoudi L. & Fagel N. (2014) Mineralogical and geotechnical characterization of clays from northern Morocco for their potential use in the ceramic industry. *Clay Minerals*, **49**, 35–51.

Felhi M., Tlili A., Gaied M.E. & Montacer M. (2008) Mineralogical study of kaolinitic clays from Sidi El Bader in the far north of Tunisia. *Applied Clay Science*, **39**, 208–217.

Földvári M. (2011) *Handbook of the Thermogravimetric System of Minerals and Its Use in Geological Practice*. Budapest, Hungary. Geological Institute of Hungary, 180 pp.

Geological Society of America (2009) *Geological Rock-Color Chart with Genuine Munsell Color Chips. Revision of the Previously Published Geological Society of America (GSA) Rock-Color Chart Prepared by the Rock-Color Chart Committee*. Grand Rapids, MI, USA, Munsell.

Greene-Kelly R. (1957) The montmorillonite minerals. Pp. 140–164 in: *The Differential Thermal Investigation of Clays* (R.C. Mackenzie, editor). London, UK, The Mineralogical Society.

Grim R.E. & Rowland R.A. (1944) Differential thermal analysis of clays and shales, control and prospecting method. *Journal of the American Ceramic Society*, **27**, 65–76.

Grim R.E. (1953) *Clay Mineralogy*. New York, NY, USA, McGraw-Hill, 384 pp.

Güven N. (2001) Mica structure and fibrous growth of illite. *Clays and Clay Minerals*, **49**, 189–196.

Hammami-Ben Zaied F., Abidi R., Slim-Shimi N. & Somarin A.K. (2015) Potentiality of clay raw materials from Gram area (northern Tunisia) in the ceramic industry. *Applied Clay Science*, **112–113**, 1–9.

Holtz R.D. & Kovacs W.D. (1981) The relationship between geology and landslide hazards of Atchison, Kansas and Vicinity. *Current Research in Earth Sciences*, **244**, 1–16.

Joussein E., Petit S., Churchman J., Theng B., Righi D. & Delvaux B. (2005) Halloysite clay minerals – a review. *Clay Minerals*, **40**, 383–426.

Kamseu E., Leonelli C., Boccaccini D.N., Veronesi P., Miselli P., Giancarlo Pellacani G. & Chinje Melo U. (2007) Characterisation of porcelain compositions using two china clays from Cameroon. *Ceramics International*, **33**, 851–857.

Kreimeyer R. (1987) Some notes on the firing colour of clay bricks. *Applied Clay Science*, **2**, 175–183.

https://doi.org/10.1180/clm.2019.49 Published online by Cambridge University Press

Laboratoire Central des Ponts et Chaussées (1987) *Limites d'Atterberg, limite de liquidité, limite de plasticité, method d'essai LPC, no. 19*. Paris, France, Publication LCPC, 26 pp.

Mahmoudi S., Srasra E. & Zargouni F. (2008) The use of Tunisian Barremian clay in the traditional ceramic industry: optimization of ceramic properties. *Applied Clay Science*, **42**, 125–129.

McManus J. (1988) Grain size distribution and interpretation. Pp. 63–85 in: *Techniques in Sedimentology* (M.E. Tucker, editor). Oxford, UK, Blackwell.

Milošević M. & Logar M. (2017) Properties and characterization of a clay raw material from Miličinica (Serbia) for use in the ceramic industry. *Clay Minerals*, **52**, 329–340.

Milošević M., Logar M., Kaluđerović L. & Jelić I. (2017) Characterization of clays from Slatina (Ub, Serbia) for potential uses in the ceramic industry. *Energy Procedia*, **125**, 650–655.

Minato H. & Shibue Y. (1999) A case for utilization of clays to raw materials of outside wall at final disposal site of town waste matters and new treatment techniques for pollution soils. *Clay Science*, **38**, 167–180.

Mitrović A.A., Komljenović M.M. & Ilić B.R. (2009) Ispitivanja mogućnosti korišćenja domaćih kaolinskih glina za proizvodnju metakaolina. *Hemijska Industrija*, **63**, 107–113.

Mojsilović S., Baklajić D., Đoković I. & Avramović V. (1971) Tumač za list Titovo Užice K. 34-4. Pp. 30–49 in: *Zavod za Geološka i Geofizička Istraživanja* (M. Dimitrijević *et al*., editors). Belgrade, Serbia, NIGP 'Privredni pregled'.

Monterio S.N. & Vieira C.M.F. (2004) Influence of firing temperature on the ceramic properties of clays from Campos dos Goytacazes, Brazil. *Applied Clay Science*, **27**, 229–234.

Moreno-Maroto J.M. & Alonso-Azcárate J. (2018) What is clay? A new definition of 'clay' based on plasticity and its impact on the most widespread soil classification systems. *Applied Clay Science*, **161**, 57–63.

Murray H.H. & Kogel J.E. (2005) Engineered clay products for the paper industry. *Applied Clay Science*, **29**, 199–206.

Murray H.H. (1991) Overview – clay mineral applications. *Applied Clay Science*, **5**, 379–395.

Murray H.H. (2007) *Applied Clay Mineralogy, Volume 2: Occurrences, Processing and Applications of Kaolins, Bentonites, Palygorskite-Sepiolite, and Common Clays*. Amsterdam, The Netherlands, Elsevier, 188 pp.

Newman A.C.D. (1987) Chemistry of clays and clays minerals, Pp. 2–128 in: *The Chemical Constitution of Clays* (A.C.D. Newman, editor). Mineralogical Society Monograph. London, UK, Longman.

Norton F.H. (1970) *Fine Ceramics Technology and Applications*. New York, NY, USA, McGraw-Hill, 507 pp.

Norton P.H. (1939) Critical study of the differential thermal method for identification of clay minerals. *Journal of the American Ceramic Society*, **22**, 54–63.

Reeves G.M., Sims I. & Cripps J.C. (2006) *Clay Material Used in Construction*. Special Publication no. 21. London, UK, The Geological Society, 552 pp.

Rivi A. & Ries B. (1997) Single-line dry grinding technology. *Ceramic World*, **24**, 132–141.

Sherman G.D. (1952) The titanium content of Hawaiian soils and its significance. *Soil Science Society of America Proceedings*, **16**, 15–18.

Sikalidis C.A., Kafritsas J.A. & Alexiades C.A. (1989) Kaolins of Lesbos and their suitability for the ceramics industry. *Interceramics*, **38**, 11–14.

Singh B. & Gilkes R.J. (1992) An electron optical investigation of the alteration of kaolinite to halloysite. *Clays and Clay Minerals*, **40**, 212–229.

Speil S., Berkelhamer L.H., Pask J. & Davies B. (1945) *Differential Thermal Analysis of Clays and Aluminous Minerals*. U.S. Bureau of Mines, Paper #664. Washington, DC, USA, US Government Printing Office.

Strazzera B., Dondi M. & Marsigli M. (1997) Composition and ceramic properties of Tertiary clays from Southern Sardinia (Italy). *Applied Clay Science*, **12**, 247–266.

Tsozué D., Nzeugang A.N., Macheb J.R., Loweh S. & Fagel N. (2017) Mineralogical, physico-chemical and technological characterization of clays from Maroua (Far-North, Cameroon) for use in ceramic bricks production. *Journal of Building Engineering*, **11**, 17–24.

Viseras C., Aguzzi C., Cerezo P. & Lopez-Galindo A. (2007) Uses of clay minerals in semisolid health care and therapeutic products. *Applied Clay Science*, **36**, 37–50.

Yariv S. (2003) Differential thermal analysis (DTA) in the study of thermal reactions of organo-clay complexes. Pp. 253–296 in: *Natural and Laboratory-Simulated Thermal Geochemical Processes* (R. Ikan, editor). Dordrecht, The Netherlands, Springer.

https://doi.org/10.1180/clm.2019.49 Published online by Cambridge University Press